2023 IEEE CHILEAN Conference on Electrical, Electronics Engineering, Information and Communication Technologies (CHILECON) | 979-8-3503-6953-3/23/$31.00 ©2023 IEEE | DOI: 10.1109/CHILECON60335.2023.10418600

# Hybrid Modulation Strategy for DC-Bias Current Mitigation in Dual Active Bridge Converters

Carlos Matus
*Department of Electrical Engineering*
*Universidad de La Frontera*
Temuco, Chile
c.matus07@ufromail.cl

Hector Young
*Department of Electrical Engineering*
*Universidad de La Frontera*
Temuco, Chile
hector.young@ufrontera.cl

Christian A. Rojas
*Department of Electronic Engineering*
*Universidad Tecnica Federico Santa Maria*
Valparaiso, Chile
c.a.rojas@ieee.org

Raul Opazo
*Department of Electrical Engineering*
*Universidad de La Frontera*
Temuco, Chile
r.opazo04@ufromail.cl

***Abstract*—The use of the dual active bridge (DAB) as an electronic power converter in electric vehicles has gained interest in recent years thanks to features such as bidirectional power flow, galvanic isolation, high efficiency, high power density, low component stress, among others. Phase-shift modulation schemes are widely used for DAB control, being the most basic of them the single phase shift (SPS), followed by modulations with increasing number of degrees of freedom such as the extended phase shift (EPS), dual phase shift (DPS) and triple phase shift (TPS). A relevant concern in DAB applications is the appearance of transient dc components in the transformer current which are generated by load disturbances and the resulting sudden changes in phase-shift. This dc-bias current reduces the converter efficiency, induces higher current stress in semiconductor switches and increases the risk of failures due to the saturation of magnetic cores. This paper proposes the implementation of a hybrid modulation strategy which combines different phase shift modulation schemes to mitigate the dc bias of the transformer current under load impacts. The validation of the modulation scheme is done through simulation analysis with the PLECS software.**

***Index Terms*—Dual Active Bridge (DAB) converter, dc-bias current, phase-shift modulation.**

## I. Introduction

RECENT advances on electric propulsion for vehicles, motivated by the need to reduce pollutant gas emissions, have fostered the adoption of high-efficiency and high-power-density electronic power converters. The Dual Active Bridge (DAB) converter has gained interest due to advantages such as bidirectional power transfer, galvanic isolation, and the possibility of soft switching [1], [2]. The DAB is currently applied in diverse sectors of the industry such as aerospace, renewable energy, cells for modular converters in high-power systems and electric vehicles [3]–[6].

Several modulation schemes can be applied for controlling the DAB, such as single-phase-shift (SPS), extended-phase-shift (EPS), dual-phase-shift (DPS) and triple-phase-shift (TPS) [7]. The SPS modulation works by introducing a phase shift between the gating signals of each bridge, which is called an external shift. The other modulation variants also include phase shifts between the switching signals applied to different legs in the same bridge, i.e., internal shifts. Aiming to enhance the performance of existing modulation alternatives, different modulation schemes can be combined into hybrid control strategies. The combination of phase-shift and burst-mode modulation presented in [8] allows extending the zero-voltage switching (ZVS) upon wide variations of the converter's operating conditions. A similar objective motivated the hybrid strategy developed in [2], which combines optimal solutions for the TPS modulation in order to reduce conduction and switching losses in wide operating conditions. A

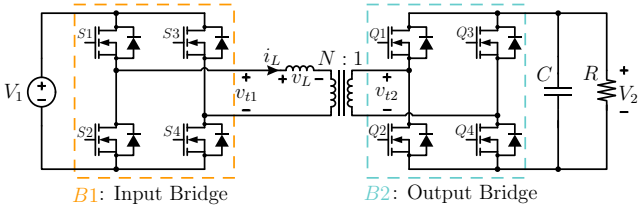


Fig. 1: Dual Active Bridge topology.

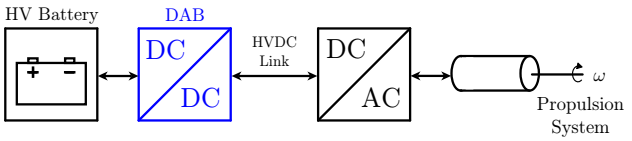


Fig. 2: Typical architecture of an electric vehicle.

This work was supported by Agencia Nacional de Investigacion y Desarrollo (ANID): AC3E (ANID/Basal/FB0008), SERC Chile (ANID/FONDAP/1522A0006), ANID through project Fondecyt 1210757 and by Project FRO19101 MINEDUC (Ministerio de Educacion, Chile)

979-8-3503-6953-3/23/$31.00 ©2023 IEEE

recent example of hybrid modulation strategies is focused on minimizing conduction losses in the transformer and power transistors, consisting on using the EPS scheme for low and medium load levels, and the SPS for high load [9].

Most of the existing hybrid strategies focus only on improving the steady-state efficiency by switching between different modulations or operation modes of the same modulation depending on the load level. However, the transient response of the electrical variables in the DAB is also relevant, specially the transient dc-bias current in the high-frequency transformer (HFT). The transient dc-bias is caused by temporary volt-second imbalance brought by sudden phase-shift changes and its negative effects include reduced efficiency, higher current stress in semiconductor switches and premature failure of the converter due to saturation of magnetic cores [10], [11]. A conventional method to deal with dc-bias currents is the use of dc-blocking capacitors, but this solution increases the volume and cost of the converter [12]. Other mitigation strategies are based on limiting the rate of change of phase shifts according to preset current thresholds [13]. In [14] the update times of phase shifts are identified as a critical factor in the generation of transient dc-bias and a synchronization scheme is proposed to apply phase-shift updates at the exact time required to eliminate the dc-bias. Moreover, [15] proposes a strategy using an auxiliary variable in the modulation process, that allows compensating the dc bias current in transient operation.

This paper presents a study of the effect of modulation changes under transient regime and proposes a hybrid modulation strategy with the objective of reducing the dc component of the transformer current during transient operation introduced by load changes. The effectiveness of the proposed method is evaluated using simulation results.

This paper is structured as follows. First, in section II, the DAB converter topology and its modulation are presented. Then, section III presents the proposed hybrid control strategy. Section IV presents the simulation results. Finally, section IV summarizes the contribution of this paper.

## II. Dual Active Bridge (DAB)

### A. Topology description

Fig. 1 shows a diagram of the DAB topology, which consists of two full bridges connected to each other by an HFT and a series inductor which is employed for temporary energy storage and power transfer.

The DAB can operate either in boost or buck mode. Boost mode occurs when the power flows from the low-voltage side to the high-voltage side, extracting the energy from the battery. In the buck mode, the power flow is in the opposite direction and the energy is extracted from the high-voltage bridge to store energy in the battery. In this study the application context is referred to DC/DC power conversion in electric vehicles as depicted in Fig. 2, where the main task of the DAB is to enable the bidirectional power transfer between batteries and the dc-link of the inverter feeding the AC machine in the electric powertrain.

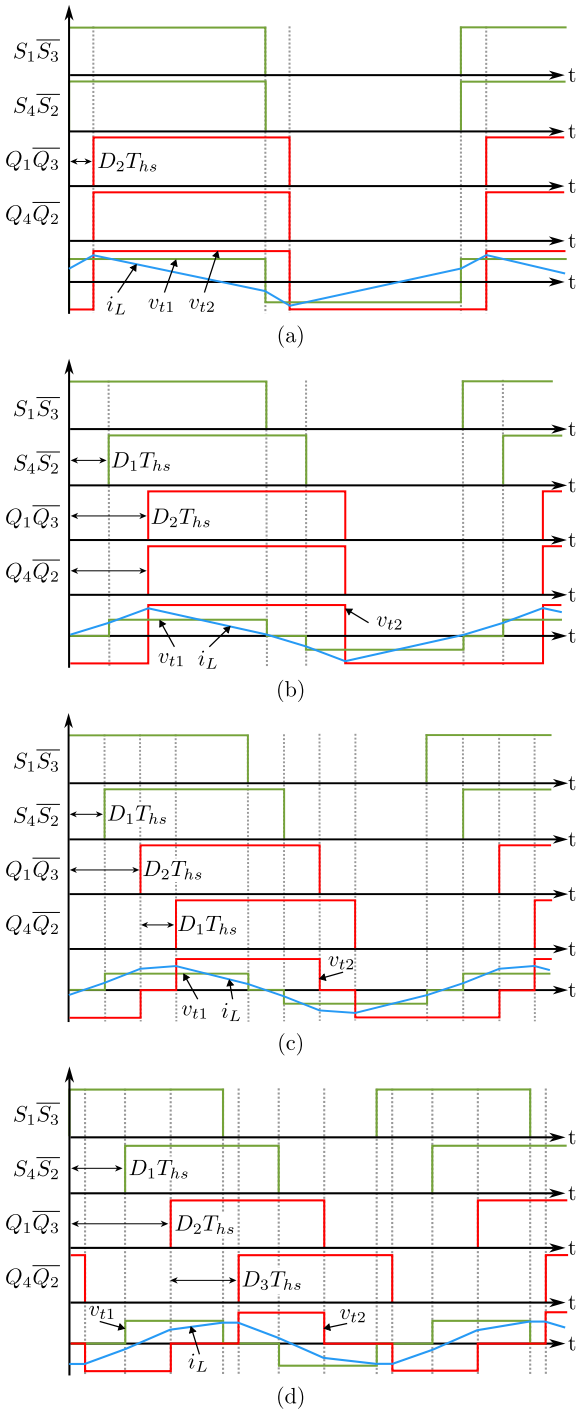


Fig. 3: Waveforms of conventional DAB modulations: (a) SPS, (b) EPS, (c) DPS and (d) TPS.

### B. DAB modulation

*1) Single Phase-Shift (SPS):* SPS is the most simple modulation scheme and consists in applying a phase shift ($D_2$) between the gating signals of both bridges, i.e., between $S_1$ and $Q_1$ as defined in Fig. 3(a). However, this modulation has some drawbacks such as a reduced ZVS range if the voltage ratio between input and output is not around unity [16].

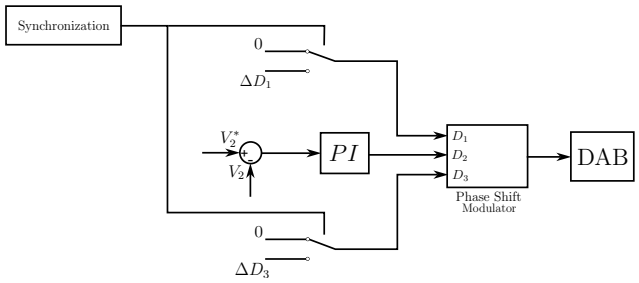


Fig. 4: Block diagram of the control scheme for the DAB.

TABLE I: DAB parameters

| Description | Parameter | Value |
|---|---|---|
| Input voltage | $V_1$ | 100 V |
| Output voltage | $V_2$ | 200 V |
| Switching frequency | $f_{sw}$ | 100 kHz |
| HFT turn ratio | $N$ | 1/2 |
| Primary side inductor | $L$ | 2.5 $\mu$H |
| Load capacitor filter | $C$ | 10 mF |

Fig. 3(a) shows waveforms of the gating signals of the power switches, the voltages of both bridges ($v_{t1}$ and $v_{t2}$) and the inductor current ($i_L$). The phase-shift applied between both bridges, measured with respect to the gating signal $S_1$, is represented as $D_2T_{hs}$, where $T_{hs}$ is half the switching period. The transmitted power with the SPS modulation can be calculated using [17]:

$$P = \frac{NV_1V_2}{2f_{sw}L}D_2(1-D_2), \tag{1}$$

where $N$ is the turns ratio of the HFT, $V_1$ and $V_2$ are the input and output voltages of the respective bridges, $f_{sw}$ is the switching frequency and $L$ is the inductance of the coupling inductor.

*2) Extended Phase-Shift (EPS):* In the EPS modulation scheme, in addition to the external phase shift ($D_2$), an internal phase shift ($D_1$) is introduced between switches $S_1$ and $S_4$ of bridge $B_1$. By working with two degrees of freedom, the EPS scheme reduces the circulating energy and the switching losses when operating at medium power range [16]. Fig. 3(b) represents the waveforms of the switching signals of both bridges with EPS modulation, their respective output voltages and inductor current. The phase shift between both bridges $D_2T_{hs}$ and the internal phase shift $D_1T_{hs}$ is shown using as reference the switching signal $S_1$.

*3) Dual Phase Shift (DPS):* In the DPS scheme, another phase-shift is added between the branches of bridge $B2$. The magnitude of this phase-shift is equal to $D_1$, i.e., the phase-shift between switches $S_1$-$S_4$ and $Q_1$-$Q_4$ is the same. The basic waveforms of DPS modulation are presented in Fig. 3(c).

*4) Triple Phase-Shift (TPS):* The TPS modulation operates similarly to the DPS, being the main difference the independent magnitude of the internal phase-shift in bridges $B_1$ and $B_2$. TPS has three degrees of freedom, as represented in the waveforms of Fig. 3(d), meaning that SPS, EPS and DPS can be seen as particular cases of the TPS modulation. The advantages of TPS are an increased converter performance, reduced RMS values of the current and increased possibilities for soft switching operation [16].

## III. Proposed hybrid control strategy

### A. Control layout

The proposed hybrid modulation strategy consists in a controlled switching of the modulation scheme applied to the DAB upon events of load disturbance, i.e., under transient regime. The control scheme shown in the block diagram of Fig. 4 consists in a voltage control loop with a reference $V_{ref}$ and feedback of the output voltage of bridge $B_2$. The external phase-shift $D_2$ is generated by a proportional-integral (PI) controller, followed by the phase-shift modulator (PSM), which produces the switching signals for the DAB switches. The internal phase-shifts $D_1$ and $D_3$ are set as constants ranging between 0 and 1, defined according to the employed modulation scheme [16]. Table I summarizes the DAB parameters used for implementing the simulation in PLECS.

### B. Computation of internal phase-shifts

In terms of their degrees of freedom, SPS, EPS and DPS can all be considered particular cases of TPS. Therefore, in this work an optimized modulation scheme based on TPS [18] is used for computing phase-shifts under different scenarios. Let us define the normalized transmitted power $P_0$ as follows:

$$P_0 = \frac{P}{P_N}, \tag{2}$$

where $P_N$ is the nominal power is given by [18]:

$$P_N = \frac{NV_1V_2}{8f_{sw}L}. \tag{3}$$

$P_0$ in (2) is defined according to the switching mode in which the DAB is operating. In this work, three switching modes are considered, which are defined from the relative values of phase-shifts $D_1$, $D_2$ and $D_3$, as detailed in Table II. Within each mode, the value of $P_0$ is computed as follows [18]:

$$\frac{P_0}{2} = \begin{cases} -D_1 + 2D_2 + D_3 - D_1^2 - 2D_2^2 + \\ -D_3^2 + 2D_1D_2 + D_1D_3 - 2D_2D_3, & \text{mode 1} \\ -D_1 + 2D_2 + D_3 - D_2^2 - D_3^2 + \\ \qquad + D_1D_3 - 2D_2D_3, & \text{mode 2} \\ -D_1 - D_3 + D_1D_3 + 1, & \text{mode 3} \end{cases} \tag{4}$$

Therefore, depending on the modulation scheme that is used, the power that is transmitted and the voltages $V_1$ and $V_2$, the values of the phase angles that comply with these restrictions can be obtained from the expressions in (4).

With the purpose of evaluating the behavior of the system under increasing changes of internal phase-shifts, the base value of these variables was set to zero, i.e., $D_1 = 0$ and $D_3 = 0$, which means that the SPS is the base modulation

TABLE II: Definition of switching modes [18]

| Mode | Constraints |
|---|---|
| 1 | $0 \leq D_1 \leq D_2 \leq D_2 + D_3 \leq 1$ |
| 2 | $0 \leq D_2 \leq D_1 \leq D_2 + D_3 \leq 1$ |
| 3 | $0 \leq D_2 + D_3 - 1 \leq D_2 \leq D_1 \leq 1$ |

scheme. Then, different sets of internal phase-shifts are established depending on the desired modulation scheme transition. In the case of changing from SPS to EPS the maximum phase-shift variation is 0.8, i.e., $\Delta D_{1,max} = 0.8$. When switching from SPS to the DPS modulation scheme, the maximum variation of both internal phase-shifts are 0.8 and 0.7, depending on the level of transmitted power.

### C. Modulation switching algorithm

To implement the switching between modulation schemes it is sufficient to change the internal phase-shift values depicted as constants $\Delta D_1$ and $\Delta D_3$ in Fig. 4, according to the required transition of modulation scheme. Considering SPS as the base modulation, to switch to EPS it is only necessary to change the value of constant $\Delta D_1$, whereas in order to switch to DPS modulation the values of $\Delta D_1$ y $\Delta D_3$ need to be adjusted to satisfy $\Delta D_1 = \Delta D_3$. These changes are introduced by using a signal switch block, controlled by a step source that represent the instant of a load impact. In practice, this signal can be generated upon detecting a load power change larger than a defined threshold.

### D. Performance evaluation

Since the objective is to reduce the dc-bias current in the HFT during a transient, the average current through the in-series inductor is selected as a measure of the performance of the proposed modulation strategy. Accordingly, the main performance criterion for the modulation schemes is the peak value of the average inductor current within one switching period, measured during a transient event:

$$\hat{I}_{L,\text{avg}} = \max\left(\left\{\frac{1}{T_s}\int_{kT_s}^{(k+1)T_s} i_L(t)dt : k = 1,\ldots,N_c\right\}\right), \tag{5}$$

where $T_s = 10\,\mu$s is the switching period and $N_c$ is the number of switching cycles required to achieve the steady state after a power disturbance.

## IV. Simulation Results

The evaluation of the proposed method was carried out by computer simulations using the PLECS software. Load impact trials were implemented by connecting resistances in parallel to achieve three load change scenarios: from 400 to 800 W, from 800 to 400 W and from 400 to 200 W. Within each load disturbance, the modulation schemes were switched from SPS to EPS and from SPS to DPS. The peak value of the average inductor current within a switching period was measured and analyzed for different variations of the internal phase-shift.

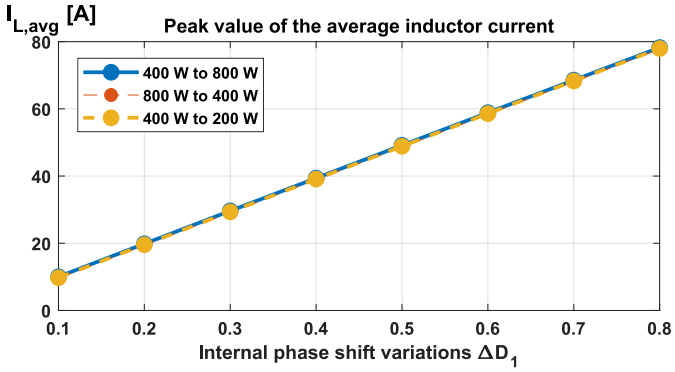


Fig. 5: Peak average inductor current in transient regime. Modulation change from SPS to EPS.

The variation of the internal phase-shift corresponds to the difference between the phase-shift before the change of the load and after the change of the load on either bridge B1 ($\Delta D_1$) or bridge B2 ($\Delta D_3$). The system is considered to be operating in steady-state with a nominal output voltage $V_2$ set to 200 V and regulated by the PI controller to maintain the nominal voltage constant under load changes.

### A. Modulation change: SPS to EPS

As can be seen in Fig. 5, the average inductor current presents a linear behavior, increasing along the variation of the internal phase-shift $\Delta D_1$. Furthermore, the simulation results show that the load level has a low impact on the result. From the definition of the working principle of the EPS modulation (Fig. 3), to introduce a phase-shift implies a change only in the internal phase-shift $D_1$ while keeping phase-shift $D_3 = 0$ permanently. That is, the following condition is satisfied: $\Delta D_1 \neq 0$ and $D_3 = \Delta D_3 = 0$. This situation explains the ineffectiveness of the EPS scheme while performing a transition from SPS under a load impact event.

### B. Modulation change: SPS to DPS

Fig. 6 presents the average inductor current at the moment of a load impact and applying at the same time the hybrid control strategy at the instant $t = 0.08$ s, with the specified internal phase-shift variations. Positive average inductor current peaks occur in the cases shown in Fig. 6 (b) and negative average inductor current peaks occur in the cases shown in Fig. 6 (a). This effect is due to the increase or decrease of the transmitted power, producing a negative peak when the power increases and a positive peak when the power decreases.

To summarize the performance of this strategy, Fig. 7 shows the peak average inductor current obtained with a change from SPS to DPS modulations versus different variations of the internal phase-shifts $\Delta D_1 = \Delta D_3$ and considering different load step changes. In comparison with the results in Fig. 5, it is clear that the change from SPS to DPS yields much lower average peak currents in all the studied cases. In Fig. 7 (a) the current decreases monotonically for increasing values of $\Delta D_1$ and $\Delta D_3$. On the other hand, in the cases presented in

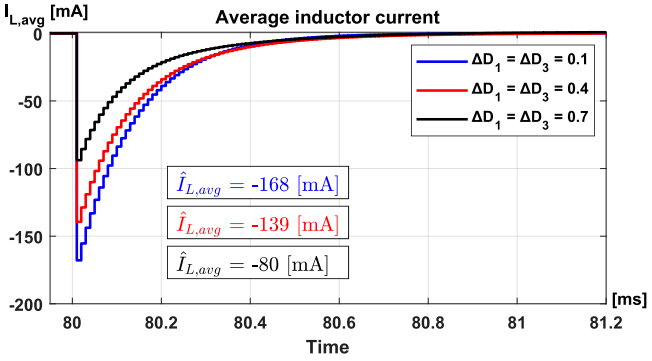


(a)

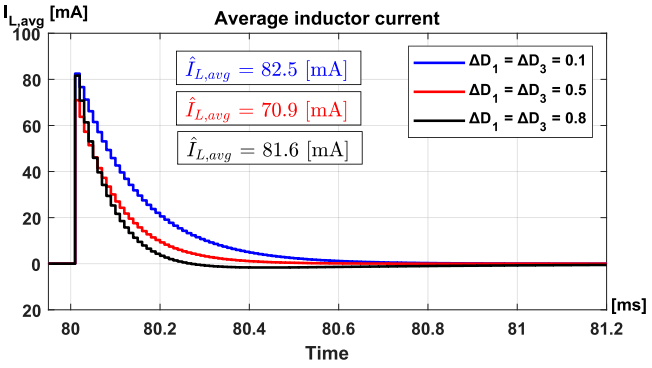


(b)

Fig. 6: Average inductor current in time for case SPS to DPS (a) 400 to 800 W; (b) 400 to 200 W.

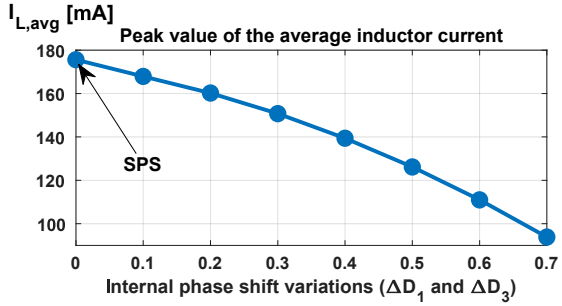


(a)

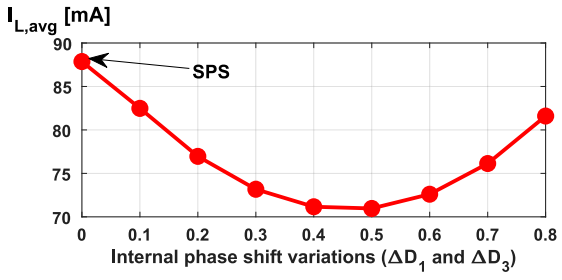


(b)

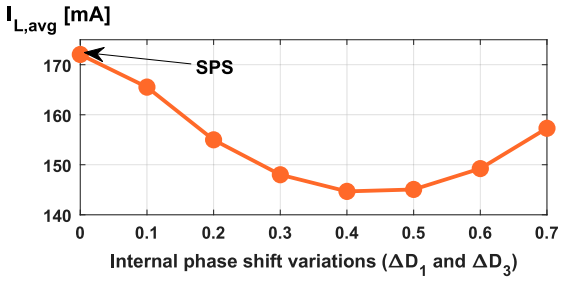


(c)

Fig. 7: Peak value of the average inductor current SPS to DPS (a) 400 to 800 W; (b) 400 to 200 W; (c) 800 to 400 W.

Fig. 7 (b) and (c), the current decreases to a minimum when $\Delta D_1 = \Delta D_3 = 0.5$.

Unlike the EPS scheme, the operation of the DPS modulation implies that both the internal phase-shifts must always have the same value, i.e., $D_1 = D_3$. Therefore, the phase-shift variations will be identical with $\Delta D_1 = \Delta D_3$. This is the reason of the noticeable advantage of the DPS scheme in the proposed modulation strategy.

These results can lead to control strategies which allow to reduce the transient dc current of the inductor, since the control of the output voltage could be carried out through a phase-shift angle, (in this case, the external phase-shift $D_2$) and use the other two phase-shift angles to decrease the average inductor current at the time of making a change in the load. Another option that could be investigated is to regulate the output voltage through the internal phase-shifts, manipulating both of them with the same output of a PI controller, and to adjust the external phase-shift in order to decrease the transient dc current of the inductor. This latter case allows taking advantage of the condition revealed in this research as the most efficient to reduce the dc-bias current during transient, which is equal variation of internal offsets at the moment of a load transient, i.e., $\Delta D_1 = \Delta D_3$.

## V. Conclusion

This paper presented a control strategy for the DAB converter based on a combination of SPS, EPS and DPS modulations aimed to reduce dc-bias currents under transient operation. Tests were carried out to verify the operation of the hybrid modulation scheme taking the peak value of the average current of the inductor as a performance criterion. From the results obtained, it can be concluded that a variation from the SPS to DPS scheme allows for lower average inductor current peak values when facing a load transient, compared to maintaining the SPS scheme or changing to the EPS scheme. The reason for these results resides in the operation of the DPS scheme, in which both internal offsets always have the same value, unlike the EPS scheme where the internal offsets have different values. Future research will consider a voltage control loop based on the internal phase-shifts of DPS while adjusting the external phase-shift to reduce transient dc-bias.

## References

[1] F. Krismer and J. W. Kolar, "Efficiency-Optimized High-Current Dual Active Bridge Converter for Automotive Applications," *IEEE Transac-*

*tions on Industrial Electronics*, vol. 59, no. 7, pp. 2745–2760, Jul. 2012.
[2] A. K. Bhattacharjee and I. Batarseh, "Optimum Hybrid Modulation for Improvement of Efficiency Over Wide Operating Range for Triple-Phase-Shift Dual-Active-Bridge Converter," *IEEE Transactions on Power Electronics*, vol. 35, no. 5, pp. 4804–4818, May 2020.
[3] Q. Bu, H. Wen, H. Shi, Y. Hu, and Y. Yang, "Universal Transient DC-Bias Current Suppression Strategy in Dual-Active-Bridge Converters for Energy Storage Systems," *IEEE Transactions on Transportation Electrification*, vol. 7, no. 2, pp. 509–526, Jun. 2021, publisher: Institute of Electrical and Electronics Engineers Inc.
[4] B. Zhao, Q. Song, J. Li, X. Xu, and W. Liu, "Comparative Analysis of Multilevel-High-Frequency-Link and Multilevel-DC-Link DC–DC Transformers Based on MMC and Dual-Active Bridge for MVDC Application," *IEEE Transactions on Power Electronics*, vol. 33, no. 3, pp. 2035–2049, Mar. 2018.
[5] L. Tarisciotti, A. Costabeber, L. Chen, A. Walker, and M. Galea, "Current-Fed Isolated DC/DC Converter for Future Aerospace Microgrids," *IEEE Transactions on Industry Applications*, vol. 55, no. 3, pp. 2823–2832, May 2019.
[6] M. Roche, W. Shabbir, and S. Evangelou, "Voltage Control for Enhanced Power Electronic Efficiency in Series Hybrid Electric Vehicles," *IEEE Transactions on Vehicular Technology*, pp. 1–1, 2016.
[7] B. Zhao, Q. Song, W. Liu, and Y. Sun, "Overview of Dual-Active-Bridge Isolated Bidirectional DC–DC Converter for High-Frequency-Link Power-Conversion System," *IEEE Transactions on Power Electronics*, vol. 29, no. 8, pp. 4091–4106, Aug. 2014.
[8] V. M. Iyer, S. Gulur, and S. Bhattacharya, "Hybrid control strategy to extend the ZVS range of a dual active bridge converter," in *2017 IEEE Applied Power Electronics Conference and Exposition (APEC)*. Tampa, FL, USA: IEEE, Mar. 2017, pp. 2035–2042.
[9] B. Liu, P. Davari, and F. Blaabjerg, "An Optimized Hybrid Modulation Scheme for Reducing Conduction Losses in Dual Active Bridge Converters," *IEEE Journal of Emerging and Selected Topics in Power Electronics*, vol. 9, no. 1, pp. 921–936, Feb. 2021.
[10] N. M. L. Tan, T. Abe, and H. Akagi, "Design and Performance of a Bidirectional Isolated DC–DC Converter for a Battery Energy Storage System," *IEEE Transactions on Power Electronics*, vol. 27, no. 3, pp. 1237–1248, Mar. 2012.
[11] H. Du and X. Wen, "Influence of DC Bias to Transformer and Its Suppression Measures," in *2011 Asia-Pacific Power and Energy Engineering Conference*. Wuhan, China: IEEE, Mar. 2011, pp. 1–4.
[12] S. Shao, L. Chen, Z. Shan, F. Gao, H. Chen, D. Sha, and T. Dragicevic, "Modeling and Advanced Control of Dual-Active-Bridge DC-DC Converters: A Review," *IEEE Transactions on Power Electronics*, vol. 37, no. 2, pp. 1524–1547, Feb. 2022, publisher: Institute of Electrical and Electronics Engineers Inc.
[13] B. Zhang, S. Shao, L. Chen, X. Wu, and J. Zhang, "Steady-State and Transient DC Magnetic Flux Bias Suppression Methods for a Dual Active Bridge Converter," *IEEE Journal of Emerging and Selected Topics in Power Electronics*, vol. 9, no. 1, pp. 744–753, Feb. 2021.
[14] S. Wang, C. Li, K. Wang, Z. Zheng, and Y. Li, "Loss Imbalance and Transient DC-Bias Mitigation in Dual-Active-Bridge DC/DC Converters," *IEEE Journal of Emerging and Selected Topics in Power Electronics*, vol. 9, no. 2, pp. 1399–1409, Apr. 2021.
[15] D. Shu, H. Wang, and M. Zhou, "Universal Control Scheme to Achieve Seamless Dynamic Transition of Dual-Active-Bridge Converters Using Zero-Current-Prediction," *IEEE Transactions on Industrial Electronics*, vol. 69, no. 6, pp. 5826–5834, Jun. 2022, publisher: Institute of Electrical and Electronics Engineers Inc.
[16] C. Calderon, A. Barrado, A. Rodriguez, P. Alou, A. Lazaro, C. Fernandez, and P. Zumel, "General Analysis of Switching Modes in a Dual Active Bridge with Triple Phase Shift Modulation," *Energies*, vol. 11, no. 9, p. 2419, Sep. 2018.
[17] N. Noroozi, A. Emadi, and M. Narimani, "Performance Evaluation of Modulation Techniques in Single-Phase Dual Active Bridge Converters," *IEEE Open Journal of the Industrial Electronics Society*, vol. 2, pp. 410–427, 2021.
[18] C. Song, A. Chen, J. Chen, C. Du, and C. Zhang, "Optimized modulation scheme for dual active bridge dc-dc converter," in *2018 IEEE Applied Power Electronics Conference and Exposition (APEC)*. San Antonio, TX, USA: IEEE, Mar 2018, p. 3569–3574.